Environmental Science
Water Research & Technology

ROYAL SOCIETY OF CHEMISTRY

PAPER

View Article Online
View Journal | View Issue

Cite this: *Environ. Sci.: Water Res. Technol.*, 2026, **12**, 1021

Quantifying the hydraulic conditions that govern discolouration material behaviour in drinking water distribution systems

Reinar Lokk, *[a] Joby Boxall [b] and Stewart Husband [b]

Recurring consumer complaints of discoloured water indicate a key management challenge for drinking water distribution systems (DWDS). This research examines the causes by investigating and quantifying the impacts of hydraulic conditions on the transition of material between the bulk water and infrastructure surfaces. It is the first to acknowledge and differentiate between particulate accumulation and mobilisation due to the processes of sedimentation and cohesive layers and provide evidenced based operation and maintenance guidelines to improve discolouration management. With the range of physical, chemical and biological interactions within DWDS the specific processes enabling particles to remain on pipe surfaces are not investigated or quantified here with the focus on delivering evidence based practical support. Results from 8 independent week long trials incorporating 18 hydraulic profiles in a full sized and extensively monitored experimental pipe-loop with flow control precision of 0.002 m s^{-1} and using discolouration material collected from multiple operational networks are presented. Reynolds number is proposed to best describe the limit of sedimentation as a measure of the turbulence forces that are balanced by the self-weight forces. Shear stress, that quantifies surface forces, is proposed to best describe mobilisation. For practical guidelines and uptake these can be converted to velocities. Sedimentation was found to dominate up to a Reynolds number of 15 100 (0.25 m s^{-1}, 0.21 N m^{-2}); above this cohesive layers were dominant. This indicates discolouration risks from sedimentation, likely in the tertiary zones of a DWDS, may be mitigated if flows regularly attain these values. Material accumulated following sedimentation was shown to be effectively removed by a shear stress of 0.77 N m^{-2} (0.5 m s^{-1}, Re 30 300), representing an idealised flushing value as forces above this showed negligible benefit on their removal. No effective upper flushing value was found in these trials for effective full mobilisation of cohesive layers.

Received 7th September 2025,
Accepted 8th January 2026

DOI: 10.1039/d5ew00873e

rsc.li/es-water

Water impact

Discolouration in drinking water networks remains a key challenge for utilities. This study quantifies, for the first time, the hydraulic thresholds that govern sedimentation and cohesive layer dominance, using full-scale experiments. The findings provide evidence-based guidelines for network design, operation, and flushing strategies to improve water quality and reduce discolouration risk.

1. Introduction

Discolouration of drinking water is not a new phenomenon but despite the health, financial and regulatory motivators it continues to occur across distribution networks. Discolouration can be described as a two-phase process: firstly particles accumulating on pipe surfaces; and secondly mobilisation. For discolouration to be observed these processes must be in sufficient quantities for high turbidity to result. Both accumulation and mobilisation of material (*i.e.* material behaviour) leading to discolouration are primarily driven by network hydraulic conditions that are a function of pipe characteristics (*e.g.* diameter, roughness) and are often reported as flowrate, velocity or shear stress.[1–4] Material may accumulate due to sedimentation or cohesive processes.[4] Sedimentation refers to particle settling due to self-weight under gravity resulting in the formation of deposits at the pipe invert.[1,5–7] The second accumulation process involves particles forming cohesive layers on all pipe surfaces, so termed as they as exhibit a shear stress

[a] *United Utilities PLC, Lingley Mere Business Park, Warrington, UK.*
E-mail: re1nar@hotmail.com
[b] *The University of Sheffield, Western Bank, Sheffield, UK*

relationship as verified extensively in laboratory and field trials.. Although the presence and behaviour of cohesive material layers are well documented, the actual processes governing their formation are not defined with the range of physical and chemical interactions within drinking water distribution systems (DWDS) and the mutually endemic presence of biofilms all considered involved.[8–10] Previously these twin processes have been studied separately and as occurring independently. However, Boxall *et al.*[4] acknowledged that sedimentation and cohesive layers co-exist and conceptually integrated them, but lacking specification and quantification of the conditions to dictate when and where each will dominate.

Factors such as microbial interactions and biofilms, temperature, Brownian motion of smaller particles, particle flocculation, or changes in particle characteristics due to variations in water chemistry (like chlorine decay), can all impact material behaviour. Quantifying these effects is not straightforward.[11–13] In particular, biofilms are considered a key part of cohesive layers by supporting the entrainment of material in their extracellular polymeric substances (EPS) matrix.[14,15] There is a significant body of evidence that suggests hydraulic mediated processes often dominate over the above.[1,4,16,17] Hydraulic conditions are also often the most easily controlled and managed within DWDS. Therefore, the focus of this research was to explore and quantify the impact of hydraulic conditions on discolouration material behaviour. We sought to understand the impact of hydraulic conditions on material exchange between the bulk water and the pipe wall, with the aim of informing network operation to mitigate discolouration events; the specific processes enabling particles to remain on pipe surfaces, including physical, chemical or biological (including biofilms), are not investigated or quantified here.

2. Background

2.1 Discolouration material characteristics

Considering the typical 10 μm (measured as volume %) size of particles reported in DWDS, any changes in hydraulic conditions can play a significant role in influencing material behaviour.[4] Sedimentation research has traditionally focused on defining hydraulic thresholds, implying cessation of accumulation irrespective of process.[6,16–18] Whereas cohesive layer research has reported accumulation as ubiquitous, forming layers with a cohesive strength greater that the imposed hydraulics.[1,19–21] Given that material accumulation depends on particle characteristics and hydraulic conditions found in DWDS, it is important to note that precise hydraulic thresholds implying the cessation of either process is unlikely, underscoring the need for scrutiny when interpreting hydraulic conditions reported as distinct thresholds. Moving away from a threshold approach, Boxall *et al.*[4] introduced a conceptual framework, showcasing the relationship between hydraulic conditions and particle characteristics, with sedimentation expected towards lower hydraulic conditions and larger particles, while smaller and lighter particles and higher hydraulic conditions favour cohesive layers. The conceptual framework however lacks specific criteria or values to indicate where either process dominates, highlighting the challenge of distinguishing between the two processes and whether a clear distinction can, or should be made.

2.2 Hydraulic conditions impacting material behaviour

Explaining material behaviour solely through sedimentation, Ryan *et al.*[6] used discolouration material (average size 15–20 μm – volume %) collected from live distribution systems in an experiment and reported that material can accumulate as sediments when velocities are below 0.06 m s^{-1}. This was supported by Vreeburg and Boxall[1] and van Thienen *et al.*,[22] who reported results from experiments using high concentration of ferric hydroxide particles and noted sediments forming at the bottom of the pipe below 0.06 m s^{-1}. Both studies however used a benchtop pipe loop system with a short straight pipe length, sharp bends and/or fittings in their experiments which can introduce unrepresentative turbulence effects impacting material behaviour.

A laboratory study by Poças *et al.*[18] reported that material can accumulate as sediments at a velocity of 0.04 m s^{-1}, and that low velocities rather than stagnation velocities actually enhanced the rate of material accumulation. The laboratory setup used by Poças *et al.*[18] was again a short pipe length benchtop system, loaded with high concentrations of sand, which served to enhance particle accumulation by providing coarse, high-surface-area media for suspended particles to attach to. The sand comprised relatively large (1200 μm) and high-density grains, promoting more frequent particle–surface interactions and accelerated deposition of small particles from bulk water to the sand bed.

Further uncertainty about the hydraulic conditions required for sedimentation to occur arises from a series of experiments in a full-scale DWDS pipe loop system at Queen's University (Canada). Braga *et al.*[3] reported the accumulation rate in their system was consistent at different velocities (0.07 m s^{-1} and 0.15 m s^{-1}) when continuously fed from their local water supply. It was suggested that this lack of difference could be linked to the high background chlorine levels that may have hindered biofilm formation and, consequently, affected material behaviour. In their subsequent experiments using coupons Braga and Filion[7,17,23] noticed particle coverage only at the pipe invert position at velocities up to 0.3 m s^{-1}, that although acknowledging cohesive layers, they suggested indicated only gravitational sedimentation occurring. It should be noted that they inoculated known size (average particle diameter 18 μm) iron oxide particles as high concentration plumes that may not reproduce the behaviour of the complex mixture and low background concentrations comprising network discolouration material.[7,17,23]

Another velocity threshold of 0.2–0.25 m s^{-1} was determined from research in the Netherlands aimed at targeting diurnal peak demands within DWDS to prevent sediment accumulation.[16,24] This threshold is often referred to as "self-cleaning" velocity implying a point where pipes are presumed to be kept "clean" – *i.e.* material is prevented from accumulating. By focussing on sediments, this assumption overlooks the existence of cohesive material layers, which have been observed well above this threshold.[19,21,25] While the "self-cleaning" concept will affect material layers by conditioning them to a set hydraulic strength, it effectively ignores their presence, thus the name "self-cleaning" can be interpreted as misleading. Whilst the concept has been reported to reduce material accumulation in Dutch networks,[26] it has not yet been shown to work in other countries with different water chemistry, particles and network hydraulics. For example, the self-cleaning velocity threshold was covered by experiments by Braga and Filion[17] where they report exponential deposition in their full scale pipe-loop of iron oxide particles, noting that velocity increase from 0.07 m s^{-1} to 0.3 m s^{-1} only produced a 6% reduction in the fraction of particles accumulated.

Model fitting to field trials investigating cohesive behaviour suggested a shear stress limit (maximum strength) of 1.2 N m^{-2} to simulate the presence of material layers in smaller diameter (<150 mm or 6″) plastic pipes. Above this value material had been effectively exhausted.[19,27] Later field trials suggested a limit of 0.7 N m^{-2} in plastic pipes.[25] Laboratory experiments by Sharpe *et al.*[21] in a plastic pipe loop system at the University of Sheffield reported that increasing daily shear stress resulted in less material accumulation by material layers and during flushing trials an excess shear stress of 3 N m^{-2} was required to remove all the mobilisable material. It was however noted that although no further material was being mobilised there remained material on the pipe walls, that is the pipe could not be fully cleaned using hydraulic strategies. This mix of results shows that whilst imposed shear stress is a factor for cohesive layer mobilisation, the daily hydraulic conditions, pipe type and material composition can all impact behavioural thresholds.

Previous studies have generally investigated sedimentation risk without considering the simultaneous occurrence of cohesive layers and *vice versa*. A review of current literature highlights that the hydraulic conditions where sedimentation or cohesive layers occur overlap, and that where and when which might dominate remain unknown. This mix of results is summarised in Table 1.

This study aimed to bridge the knowledge gap by considering the simultaneous processes of sedimentation and cohesive layer formation, identifying the dominant process, and quantifying the hydraulic conditions that influence material accumulation and mobilisation. Given the range of particle characteristics and sizes present in DWDS, it is unlikely that distinct threshold values for material behavioural shifts associated with sedimentation and cohesive layer formation can be identified. Instead, this research acknowledges the concurrent nature of both processes and, through controlled laboratory experiments imposing different hydraulic conditions, sought to determine the hydraulic conditions and parameters when either process dominates the turbidity response. The underlying premise was that the imposed hydraulic conditions would drive observable shifts between sedimentation-dominated and cohesive-layer-dominated behaviour and that identifying these shifts would provide practical insight for operational management of drinking water systems.

3. Methods

3.1 Experimental setup & plan

In order to observe discolouration behaviour and to determine the impact of hydraulic conditions on material accumulation and mobilisation processes sufficiently representatively of real systems, a full-sized pipe loop system at the University of Sheffield was used.[30] The loop consists of 200 m of 79 mm internal diameter HDPE (PE100) pipe. While the pipe was in a looped/coiled configuration, the design radius curvature of 1.5 m and with each coil having ~2.7 m straight length, turbulence, centrifugal effects *etc.* are minimised. In order to recreate the wide range of hydraulic

Table 1 Summary of hydraulic conditions that have been reported to impact material behaviour

#	Metric	Reasoning	Reported threshold	Description
1	Velocity	Velocity sufficient to prevent material accumulation by sedimentation or mobilise sediments	0.04–0.06 m s^{-1}	Threshold below which sedimentation is reported to occur[1,6,18,28]
			0.2–0.25 m s^{-1}	Diurnal threshold for Dutch network design for daily mobilisation of sediments[16,24,29]
2	Shear stress $\tau = \rho g \frac{D}{4} S_0$	Hydraulic force to remove mobilisable material (not however removing all material)	[a]0.7 N m^{-2}	Identified as threshold above which significant additional discolouration material was not mobilised in plastic pipes <6″[25]
			[a]1.2 N m^{-2}	Threshold determined by modelling above which material layers in plastic pipes <6″ exhausted[19]
			[a]3 N m^{-2}	Laboratory pipe rig determined shear stress above which mobilisable material layers exhausted in 79 mm plastic pipe[21]

[a] This relates to small diameter (<6″ or 150 mm) plastic pipes; no published values for cast iron or similar rough-walled pipes.

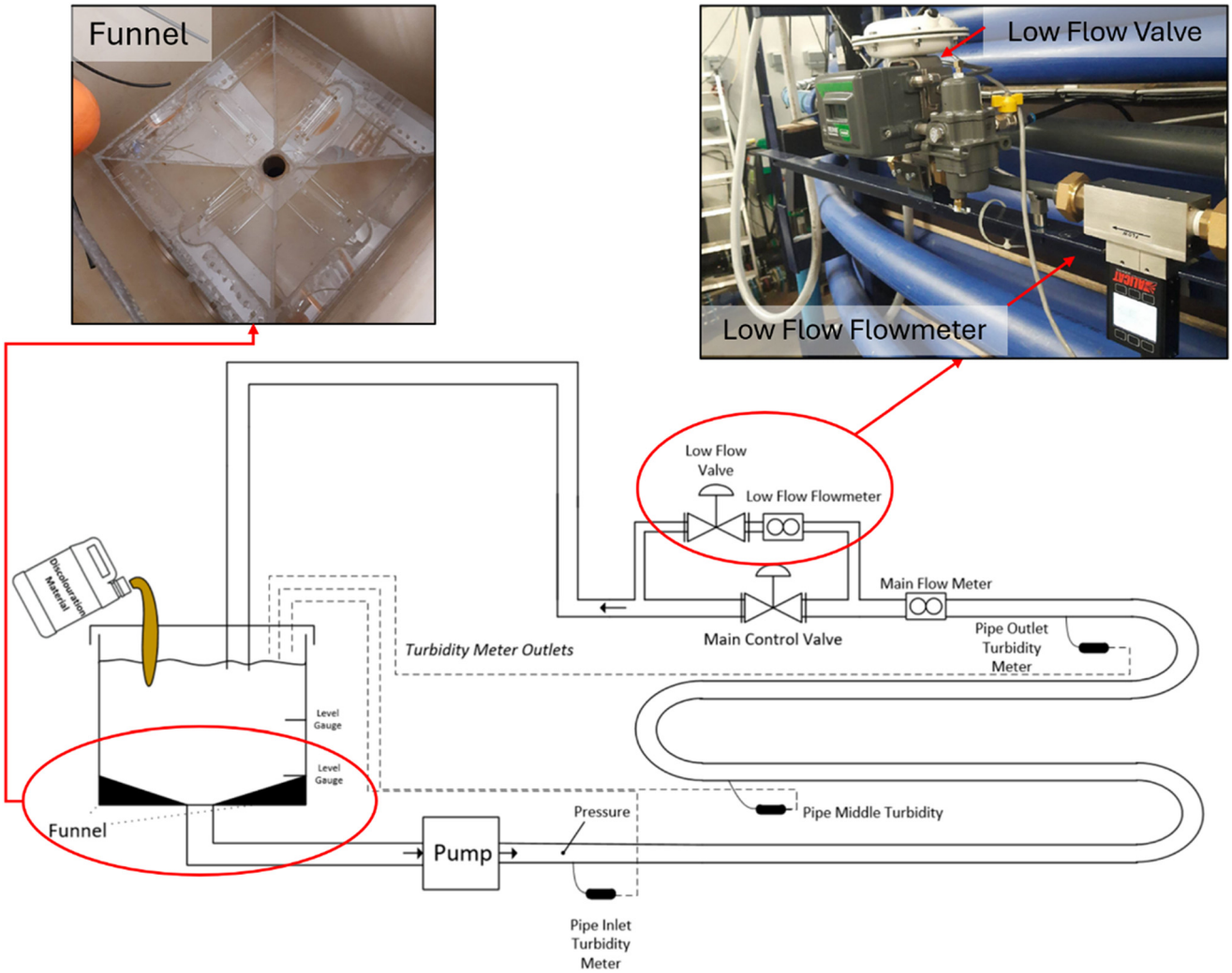

Fig. 1 Pipe loop system setup with benching and low flowrate modifications highlighted.

conditions found in DWDS, in particular the low flowrates of dead-ends that are classically associated with sedimentation, pipe loop modifications were made, as shown in Fig. 1. Modifications involved installation of a new precision control valve (Emerson Baumann 51 000) working together with the main control valve and benching (funnel) within the system tank to minimise any material accumulation within it. In order to quantify the changes in material concentrations present in the bulk water as it undergoes exchange with the system (*i.e.* pipe wall accumulation as a function of hydraulic conditions), multiple high resolution ATI A15/76 turbidity monitors were connected *via* sample lines and flow control valves (working at 0–4 NTU resolution, ±0.01 NTU). To replicate particle characteristics, discolouration material was sourced from downstream areas of DWDS (from two different UK water companies, company A and B).

In order to rigorously explore and hence understand and quantify the impact of hydraulic conditions on accumulation and mobilisation process a complex set of multiple experimental stages with multiple experimental repeats (referred to as runs) were conducted. An experimental stage comprised starting from a 'clean' system, then introducing material to achieve a desired turbidity after mixing in the system. An experimental run consisted of accumulation under a given fixed flowrate for an extended period, followed by stepped increases in hydraulic conditions to cause mobilisation. Flowrate was the controlled experimental variable, but this was later translated into Reynolds number, velocity and shear stress to understand which hydraulic parameter best described the observed behaviour (a pipe roughness, derived from measured head loss ≈2.8 m at 5 L s^{-1}, of k_s = 0.054 mm was used). In total 8 experimental stages were completed, each taking approximately a week to conduct. To investigate and validate different behavioural aspects, the 8 stages (S1–S8) all employed a bespoke flowrate profile with multiple repeats of the flowrate profile within the experimental stage (referred to as runs). These are detailed in Table 2 The funnel was confirmed to prevent material accumulation by secondary experiments after stages 4 and 8 where physical cleaning of the funnel surfaces to

Table 2 Experimental objectives, tasks and setting for the 8 conducted experiments

Stage	Number of runs (R1, R2 *etc.*)	Accumulation flowrates (L s^{-1})	Accumulation period (h)	Mobilisation flowrate steps (L s^{-1})	Objectives and tasks
1	3	0, 0.3	18	0.3, 0.6, 1.25, 2.5, 3.5, 5	Apply different accumulation hydraulics to determine time periods required
2	3	0, 0.3, 0.6	2	1.25, 1.75, 2.5, 5	Using determined accumulation period in stage 1 to investigate bulk water turbidity responses
3	2	0, 0.3, 1.25	2	0.3, 0.6, 1.25, 2.5, 3.5, 5	Repeat stage 2 with revised accumulation and mobilisation hydraulic conditions
4	3	0, 0.3, 1.25	2	1.25, 1.75, 2.5, 5	Repeat stage 3 with refined accumulation and mobilisation hydraulic conditions and higher material loading
5	3	0, 0.3, 1.25	2	0.3, 0.6, 1.25, 2.5, 3.5, 5	Investigate the influence of system conditions on accumulation and mobilisation by not cleaning the pipe-loop between experiments
6	2	0, 1.25	2	1.25, 1.75, 2.5, 3.5, 5	Investigate differences in accumulation and mobilisation behaviour using different discolouration material
7	1	0, 0.3, 0.6, 1.25, 2.5, 3.5, 5	2	5	Validation of accumulation hydraulic conditions determined in previous trials
8	1	0, 0.3, 1.25, 3.5, 5	2	5	Randomised accumulation hydraulic conditions to further validate findings

Overall aim: identify the dominant process and quantify the hydraulic conditions impacting material accumulation and mobilisation.

disturb any localised material had negligible turbidity response.

To ensure a consistent finishing point and mixing of discolouration material between runs within each stage a 5 L s^{-1} mixing flowrate was set (constrained by system limits). This approach was taken to ensure the mobilisation of sediments and condition material layers to a consistent shear strength (repeated between stages and runs) but acknowledging it would not remove all cohesive material layers. Due to ongoing material accumulation at higher shear strengths, it was anticipated, based on earlier research within the pipe loop and preliminary trials, that throughout each experimental stage the 5 L s^{-1} mixing flowrate would not return the system to the initial turbidity values. To obtain consistent starting conditions and to address ongoing accumulation of material into cohesive layers (and subsequent reduction in bulk water turbidity) between stages, the system was dosed (for 24 h) and then flushed with high chlorine (20 mg L^{-1} sodium hypochlorite solution) concentrations prior to the start of each experimental stage (note that between experimental runs, 5 L s^{-1} flowrate was used without chlorine dosing). This was not done for stages 5 and 8 to enable exploration if the material behaved differently for an "uncleaned" system and an increased likelihood of biofilm presence. Before the start of each experimental stage, chlorine concentrations in the pipe loop were measured and confirmed to be consistent with the incoming water (~0.4 mg l^{-1}), although this gradually decreased over the week-long experimental stages to zero.

The flowrates for accumulation and mobilisation were selected to cover the full range indicated from literature. 0 L s^{-1} was the lower limit used, commonly thought to be ideal for material sedimentation. 5 L s^{-1} (1 m s^{-1}) was the maximum for the system pump while maintaining a system pressure greater than 20 m (typical network design minimum). Intermediate flowrates of particular interest from literature were targeted such as 0.3 L s^{-1} (0.06 m s^{-1}) and 1.25 L s^{-1} (0.25 m s^{-1}). To cover the range comprehensively but with distinct enough steps for observable turbidity response, additional flowrate points of 0.6 L s^{-1} (0.12 m s^{-1}), 1.75 L s^{-1} (0.35 m s^{-1}), 2.5 L s^{-1} (0.5 m s^{-1}), and 3.5 L s^{-1} (0.7 m s^{-1}) were used. Flushing flowrates were maintained for a minimum of 30 minutes or 2 turnovers with the latter shown to achieve full mixing of material following mobilisation by the imposed hydraulic force.

Experimental stage 1 was used to determine the time required to observe distinct accumulation behaviour, then used in subsequent experiments. Stages 2 to 7 involved different flowrate profiles, conducting multiple repeats, altering system conditions and testing different discolouration material (company A sample used for stages 1 to 5, B for stages 6 to 8). Experimental objectives, tasks and system settings are shown in Table 2.

3.2 Discolouration material & monitoring

To obtain a measurable response to hydraulic changes, yet be representative of realistic DWDS material loading, 1 to 4 NTU (UK regulatory maximum at treatment works and customer points respectively) was targeted for the initial turbidity through controlled dosing of the discolouration material at the start of each experimental stage.

Discolouration material was collected from multiple networks in two water companies (A and B). Samples were collected during network flushing (non-unidirectional) over the first pipe turnover of target pipe lengths (loops and dead ends) from downstream regions of DWDS and combined. Composite company A sample measured ≈250 NTU (measured with 2100Q portable turbidimeter). Composite company B sample measured ≈200 NTU. To quantify

differences in particles between A and B samples and to see if the discolouration material collected during network flushing matched reported values, the particle size distributions were measured using Mastersizer 3000 employing laser diffraction.

To capture changes in material behaviour in response to incremental hydraulic changes, high frequency data was required. While measuring the suspended solids concentration (SSC) may be one of the representative measures of material in suspension,[17] it is impractical to obtain as a direct measurement at the high temporal resolution and low concentrations used in this research. To capture high temporal resolution time series data and observe changes in material behaviour patterns, this study therefore focused on turbidity which, with due care, can achieve the resolution and accuracy. Turbidity was measured using ATI A15/76 turbidity meters (5 second resolution) fed from sample lines tapped directly into the pipe loop and *via* flow control valves to retain consistent monitor conditions for all trials and instruments. These instruments have been shown to be effective in measuring turbidity in drinking water and use a 90-degree light scattering approach and high resolution (0.02 NTU).[13] Analysis of results by matching average, standard deviation and by high Pearson's correlation coefficient later showed that there was no significant difference between monitoring locations at the inlet, middle and outlet. This highlights that whilst turbidity may be considered a complex metric due to particle interactions, at the resolution required for this work the effects of particle behaviour during the trials are insignificant compared to the overall system responses observed. The outlet turbidity data was subsequently used for analysis as it is considered most suitable to capture responses and changes from the 200 m pipe length.

3.3 Analysis of turbidity data and comparison between experimental stages

To normalise the change in accumulation patterns across different starting turbidity concentrations and to reveal the conditions at which patterns in material accumulation changed, the turbidity percentage decrease and turbidity cumulative percentage change were calculated using eqn (1) and (2). To mitigate any short-term turbidity fluctuations in the 5 second data when calculating percentage changes, a 2 minute mean (24 datapoints) was calculated for the start and end (final).

$$\text{NTU decrease \%} = \frac{\overline{\text{NTU}_{t=0+2\text{min}}} - \overline{\text{NTU}_{t=\text{max}-2\text{min}}}}{\overline{\text{NTU}_{t=0+2\text{min}}}} \times 100 \quad (1)$$

$$\text{Cumulative Percentage Change}(\%) = \frac{\left(\text{NTU}_{t=i} - \overline{\text{NTU}_{t=\text{max}-2\text{min}}}\right)}{\left(\overline{\text{NTU}_{t=0+2\text{min}}} - \overline{\text{NTU}_{t=\text{max}-2\text{min}}}\right)} \times 100 \quad (2)$$

where NTU is turbidity, timestep $t = i$ refers to a point in time during the turbidity measurement period, timestep $t = 0$ refers to the starting point of the accumulation period, timestep t = max refers to the finish point of the accumulation period. $\overline{\text{NTU}_{t=\text{max}-2\text{min}}}$ refers to the final turbidity value obtained by averaging the NTU readings over a 2 minute period at the end of the accumulation period. $\overline{\text{NTU}_{t=0+2\text{min}}}$ is the initial (starting) turbidity value obtained by averaging the NTU readings over a 2-minute period at the start of the accumulation period.

Difference in the accumulation processes, due to the imposed hydraulic conditions, can be observed as changes in turbidity patterns. An exponential trend would be expected to indicate settling due to gravity and particle self-weight as larger and greater numbers of particles settle initially with the rate then slowing. A more uniform, linear change in turbidity with time during accumulation would be indicative of cohesive layer formation dominated by the process rates rather than the rate of supply or availability of material, at the low concentrations studied. The accumulation patterns were investigated using eqn (2) to calculate cumulative percentage change in turbidity for each accumulation period across different stages and runs as this normalisation allows comparison. To reduce the impact of noise and to improve the clarity of the overall behaviour, raw 5 second turbidity data was averaged over 2 minutes.

Mobilisation results were analysed by calculating the step change in turbidity in response to the imposed hydraulics conditions. These were also normalised by calculating mobilisation cumulative percentage change using eqn (3).

$$\text{Cumulative Percentage Change} = \frac{\overline{\text{NTU}^{j}_{t=2\ \text{TO}+2\text{min}}} - \overline{\text{NTU}_{t=0-2\text{min}}}}{\overline{\text{NTU}^{j=5\text{L s}^{-1}}_{t=2\ \text{TO}+2\text{min}}} - \overline{\text{NTU}_{t=0-2\text{min}}}} \times 100 \quad (3)$$

where $\overline{\text{NTU}_{t=0-2\text{min}}}$ refers to the starting turbidity of the mobilisation period (obtained by averaging the NTU readings over a 2 minute period before the start of mobilisation), $\text{NTU}^{j}_{t=2\ \text{TO}+2\text{min}}$ refers to the final turbidity of the mobilisation step at flowrate j. 2TO means the time for 2 complete turn overs of the pipe volume at the current flowrate. $\text{NTU}^{j=5\ \text{L s}^{-1}}_{t=2\ \text{TO}}$ refers to the final turbidity of the mobilisation period (at flowrate step j = 5 L s^{-1}).

4. Results

4.1 Material sizing

The results of particle size analysis for composite samples A and B are shown in Fig. 2, highlighting differences in how particle sizes are reported depending on the method used. The volume percentage is biased towards large particles while counts is biased towards smaller particles, confirming observations in previous literature.[4] Looking at volume percentage, sample B shows an increased presence

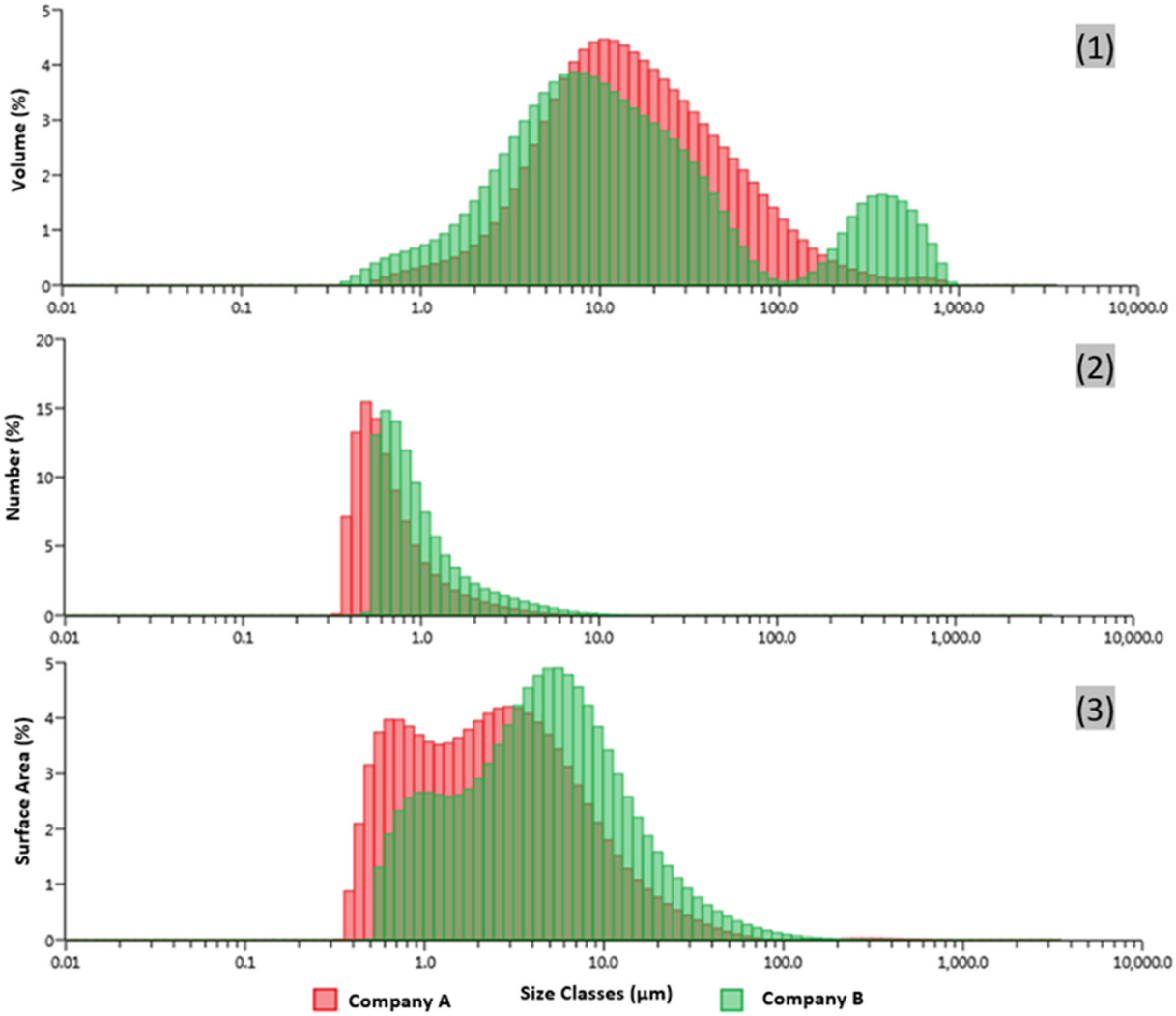

Fig. 2 Discolouration particle size analysis of company A (red) and B (green) composite samples. (1) – as volume percentage, (2) – as number percentage, (3) – as surface area percentage.

of >100 µm particles to the extent of manifesting as a very distinct bimodal distribution. When examining particle counts for both A and B samples, the presence of larger particles was inconsequential compared to particle counts below 2 µm, which constituted approximately 90% of the total particle counts for both. Surface area percentage combines the effects of count and area and revealed that particles < 10 µm were most dominant in both samples. The similarity of particle sizes based on surface area percentage suggested that the behaviour of these samples should be similar.

Both A and B composite samples corresponded with literature values of volume and counts of discolouration material sizes found in DWDS.[6,8,31,32] There is no commonly accepted technique for reporting particle size data.[33,34] From these results and analysis and consideration of literature, surface area appears to balance the bias of volume or counts and is perhaps most representative of turbidity which is measured by light scattering off surfaces. As the particles were representative of real discolouration material in drinking water distribution systems and inherently heterogeneous, with any compositional or size changes during the experiment remaining speculative (*e.g.*, through interaction with pump impellers), further particle characterisation was not undertaken as it was not required to meet the experimental aim and is complex and uncertain at the realistically low concentrations studied.

4.2 Imposed flow and bulk water turbidity

A 35 hour example of the imposed flow and turbidity measured at the inlet, middle and outlet of the pipe loop (Fig. 1) extracted from experimental stage 3 is shown in Fig. 3(A). Repeating and varied flow steps can be observed as part of the experimental design to investigate the impact of imposed hydraulics and material exchange between the bulk water and the pipe wall. It shows an expected initial differences in readings between monitor

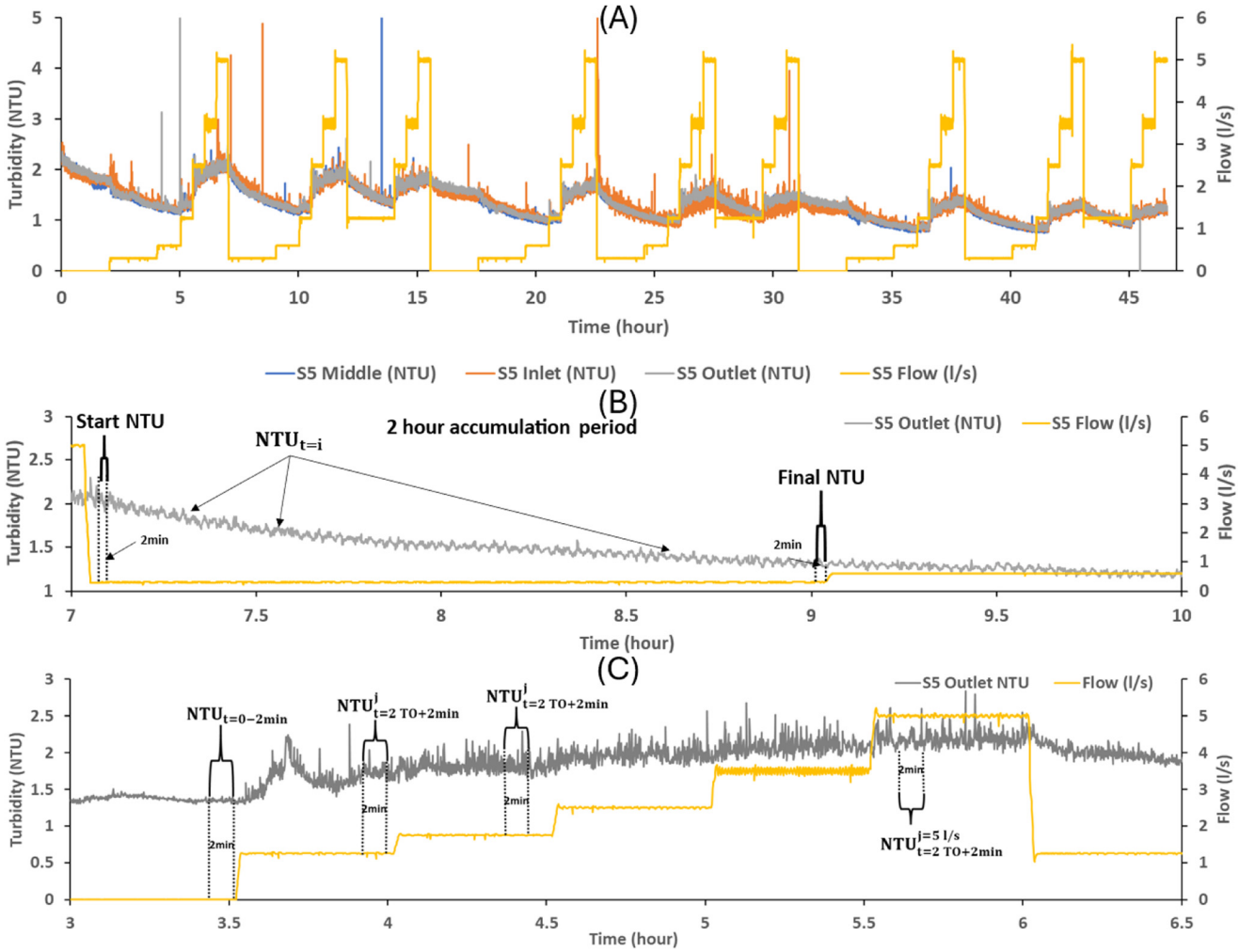

Fig. 3 Turbidity data from inlet, middle and outlet monitors and flow data during experimental stage 5 (A) with example of accumulation period data used in eqn (1) and (2) (B) and mobilisation data used in eqn (3) (C) to calculate cumulative turbidity percentage change.

locations following addition of discolouration material until system mixing and then how these are consistent throughout the experimental runs. This allows the output monitor results to be used for analysis and

Fig. 3(B) and (C) presents examples of accumulation period data used in eqn (1) and (2) (B) and mobilisation data used in eqn (3) to calculate the cumulative turbidity percentage change (C).

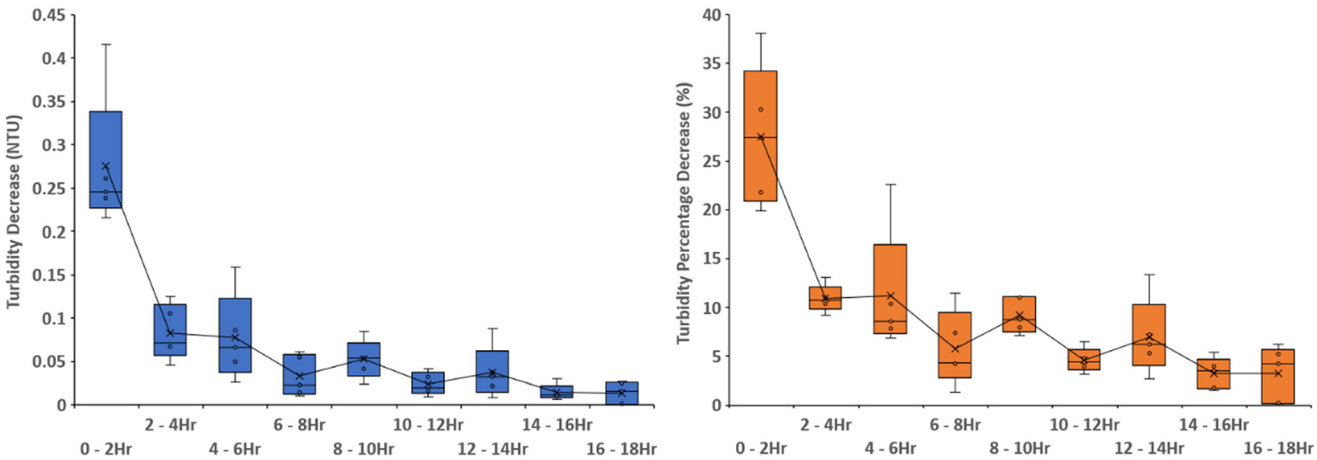

Fig. 4 Turbidity decrease (left), and turbidity percentage decrease (right) in 2 hour windows from the start of accumulation period.

4.3 Accumulation time

To confirm an appropriate experimental accumulation duration it was necessary to quantify the turbidity decay. Literature indicated that it takes approximately 2 hours for a particle of 10 μm and a density of 1200 kg m^{-3} to settle 100 mm,[35] similar to the particles used in this study and 79 mm internal experimental pipe diameter. Based on this the turbidity decrease was calculated for every 2 hours, theoretically providing each discolouration particle with adequate time to settle across the pipe diameter. As the total turbidity decease depended on background turbidity, a percentage drop was also calculated (eqn (1)) with results shown in Fig. 4. The results indicate that the greatest turbidity decay (≈30%) occurred in the first two hours and thus 2 hour accumulation period was selected for all subsequent experiments.

4.4 Accumulation patterns

Turbidity data was analysed to look for changes in patterns in turbidity decrease in response to different imposed hydraulic conditions to identify and quantify the hydraulic conditions that impacted and best described the observed accumulation behaviour. For this purpose, the total turbidity decrease over the 2 hour accumulation period was calculated, then combined across stages and runs and plotted as box plots as a function of flowrate. As the turbidity decrease is a function of initial turbidity, turbidity percentage decrease was also calculated to normalise results between stages. The results are shown in Fig. 5.

The biggest decrease and percentage decrease in turbidity was observed at a flowrate of 0.3 L s^{-1}, which was approximately 15% higher compared to the turbidity decrease at 0 L s^{-1}. In comparison to 0.3 L s^{-1}, the percentage turbidity decrease was lower (≈7%) at flow rates of 0.6 L s^{-1} and 1.25 L s^{-1}, but still higher than at 0 L s^{-1}. There was a considerable reduction in turbidity decrease between 1.25 L s^{-1} and 2.5 L s^{-1} flow rates, with the average absolute decrease dropping from 0.49 NTU to 0.14 NTU. At 5 L s^{-1}, the turbidity decrease was the smallest (0.06 NTU) and approached a negligible (with respect to measurement accuracy and replication) amount over the 2 hour accumulation period.

To identify if the hydraulic conditions impact the material accumulation processes, the change in turbidity decay patterns over the accumulation period is considered. To ensure physically meaningful comparisons across flow rates, turbidity-decay curves were fitted using linear and exponential models alongside versions of each constrained to an initial value of 100%. Fig. 6 and Table 3 reveal an initial rapid decay in turbidity at the onset followed by a more gradual decline when examining the three lower flows of 0, 0.3, and 0.6 L s^{-1}. An exponential trend described this data well suggesting that sedimentation processes were dominating under these hydraulic conditions.

At 2.5 L s^{-1} and 5 L s^{-1} the distinctive more rapid decay at the start of the accumulation period is notably absent. Because exponential fit cannot be applied to negative values, noise-induced negative turbidity values at higher flow rates were substituted with 0.01, leading to a modest bias toward exponential behaviour for flows above 1.25 L s^{-1} (when this behaviour had greatest impact). Despite this, a linear fit best describes the data at these hydraulic conditions. With only a ≈0.06 NTU and ≈0.14 NTU change in turbidity at 5 L s^{-1} and 2.5 L s^{-1} respectively, these higher flows and instrument sensitivity result in amplification of short-period oscillations in the 5 s signal, reflecting the turbulent and mixing conditions in the 200 m loop. This artefact is visible in Fig. 6. To avoid over-interpreting this short period variability, 2 minute mean values were applied for trend analysis. This more linear response indicates steady but a lower level of accumulation most likely associated with cohesive layers processes. At 1.25 L s^{-1} flowrate, the R^2 values for linear and exponential fits were closely aligned, suggesting a transition point with neither process clearly dominating.

When fixing the intercept at 100% as the start of the turbidity decay, Table 3 and Fig. 6 show that under lower-flow conditions (0–0.6 L s^{-1}), the constrained exponential model produced nearly identical fits and R^2 values to the unconstrained exponential model. This indicates that the data follows an exponential decay, supporting sedimentation

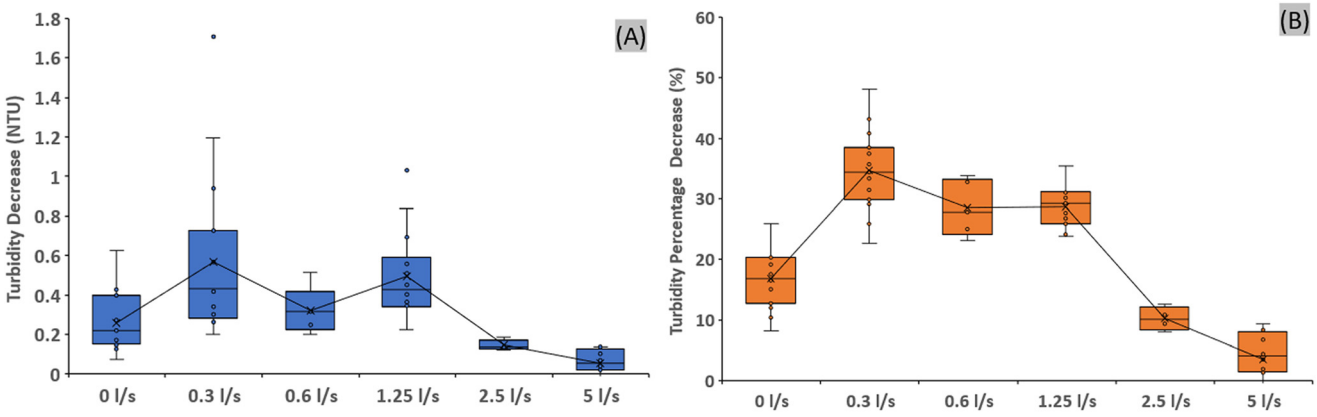

Fig. 5 Total turbidity decrease (A), and turbidity percentage decrease (B) for every 2 hour accumulation run as a function of imposed flowrate.

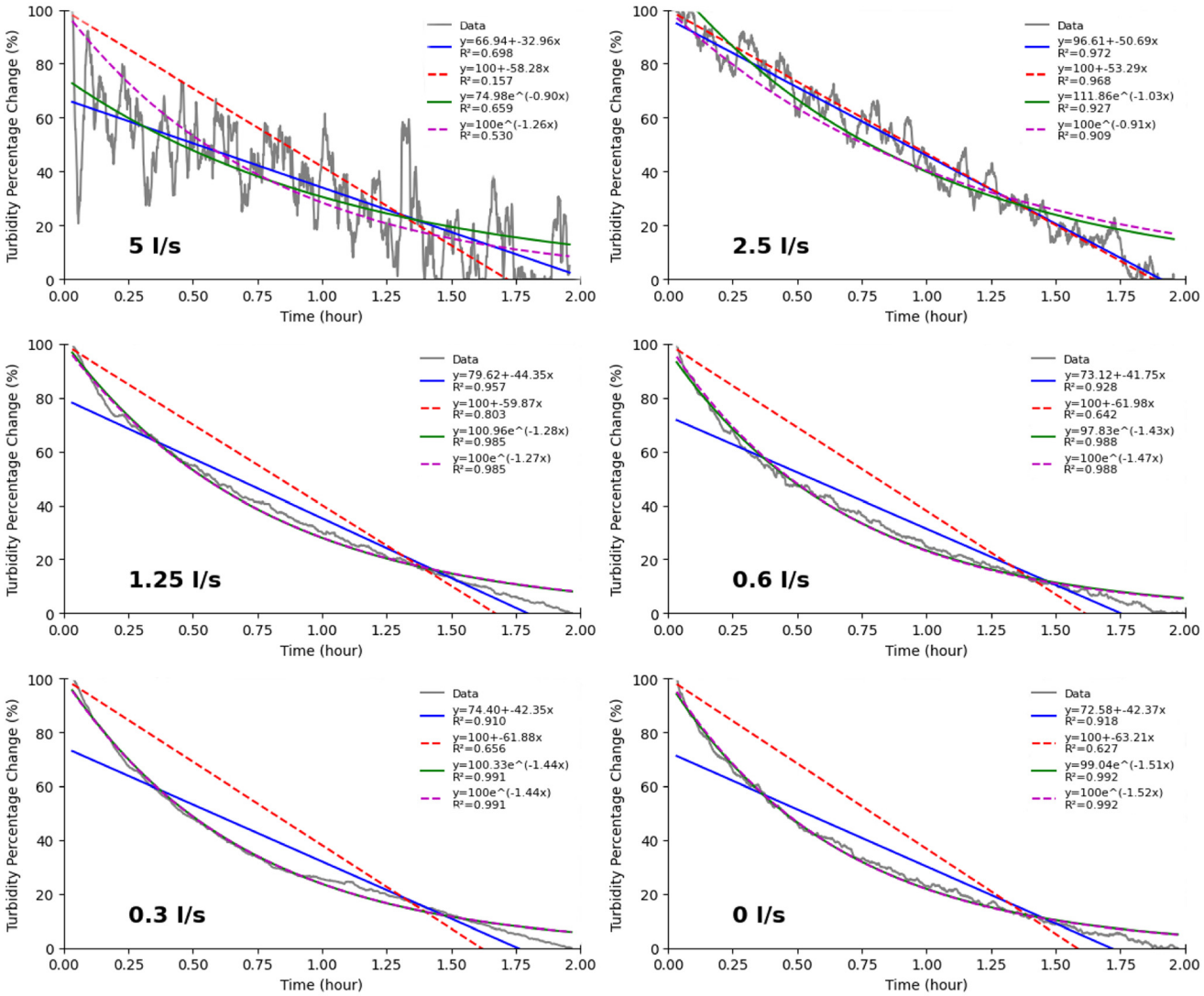

Fig. 6 Combined turbidity percentage change based on 2 min average accumulation data for all accumulation flowrates. Equations are shown for best fit lines.

effects as dominating, and that the unconstrained intercepts were already close to physically plausible values. In contrast, constraining the linear model to a 100% intercept does not improve the fit and generally reduces R^2, reflecting that the linear form is not governed by a fixed initial condition and is less appropriate for capturing curvature of the decay at lower flows. While the constrained exponential model provides a physically consistent and robust description of settling-dominated decay, constraining the linear form offers no analytical advantage and does not reflect the underlying material behaviour.

In order to be able to understand which hydraulic parameter best described the observed behaviour and to be able to generalise and transfer results from these experiments to operational DWDS, flow rate was converted to Reynolds number, velocity and shear stress. Results are shown in Table 4. These hydraulic parameters provide further insights into the dynamics at play as they consider pipe characteristics influencing system hydraulic conditions which in turn affects material behaviour in networks.

A transition from exponential to more linear behaviour was observed when increasing the flowrate from 1.25 L s^{-1} to 2.5 L s^{-1}. The percentage reduction in turbidity was only 10%, suggesting that sedimentation is less prevalent with material accumulation now dominated by cohesive layer processes. A change in flowrate from 1.25 to 2.5 L s^{-1} corresponds to a doubling of velocity and Reynolds number (from 15 000 to 30 000), but a 72% increase in shear stress (due to the exponential scaling with respect to flow, rising from 0.213 to 0.768 N m^{-2}). This suggests shear stress is a poor measure of the imposed hydraulic conditions impact on accumulation processes. As Reynolds number provides additional information about turbulence regimes, including due to surface roughness effects, it is proposed as the most informative parameter to characterise material accumulation processes across DWDS.

Table 3 Tabulated best fit lines for all flowrates. Values in bold denote best fit lines with the highest R^2 value

Flow L s^{-1}	Linear fit	Linear fit (intercept fixed to 100)	Exponential fit	Exponential fit (intercept fixed to 100)
0	$y = 72.58–42.37x$ $R^2 = 0.918$	$y = 100–63.21x$ $R^2 = 0.627$	$\mathbf{y = 99.04 \times 10^{-1.51x}}$ $\mathbf{R^2 = 0.992}$	$\mathbf{y = 100 \times 10^{-1.52x}}$ $\mathbf{R^2 = 0.992}$
0.3	$y = 74.40–42.35x$ $R^2 = 0.910$	$y = 100–61.88x$ $R^2 = 0.656$	$\mathbf{y = 100.33 \times 10^{-1.44x}}$ $\mathbf{R^2 = 0.991}$	$\mathbf{y = 100 \times 10^{-1.44x}}$ $\mathbf{R^2 = 0.991}$
0.6	$y = 73.12–41.75x$ $R^2 = 0.928$	$y = 100–61.98x$ $R^2 = 0.642$	$\mathbf{y = 97.83 \times 10^{-1.43x}}$ $\mathbf{R^2 = 0.988}$	$\mathbf{y = 100 \times 10^{-1.47x}}$ $\mathbf{R^2 = 0.988}$
1.25	$\mathbf{y = 79.62–44.35x}$ $\mathbf{R^2 = 0.957}$	$y = 100–59.87x$ $R^2 = 0.803$	$\mathbf{y = 100.96 \times 10^{-1.28x}}$ $\mathbf{R^2 = 0.985}$	$\mathbf{y = 100 \times 10^{-1.27x}}$ $\mathbf{R^2 = 0.985}$
2.5	$\mathbf{y = 96.61–50.69x}$ $\mathbf{R^2 = 0.972}$	$y = 100–53.29x$ $R^2 = 0.968$	$y = 111.86 \times 10^{-1.03x}$ $R^2 = 0.927$	$y = 100 \times 10^{-0.91x}$ $R^2 = 0.909$
5	$\mathbf{y = 66.94–32.96x}$ $\mathbf{R^2 = 0.698}$	$y = 100–58.28x$ $R^2 = 0.157$	$y = 74.98 \times 10^{-0.90x}$ $R^2 = 0.659$	$y = 100 \times 10^{-1.26x}$ $R^2 = 0.530$

The conceptual representation capturing the findings of dominant accumulation processes as a function of Reynolds number is visualised in Fig. 7. This is conceptual as there was no direct measurement of the proportion of material accumulating due to sedimentation or the formation of cohesive layers. It is important to note that the precise boundary or proportion of sedimentation and the cohesive layers processes is unknown and may be impacted by many factors, hence Fig. 7 intentionally avoids this by using a gradient colour change around this boundary.

4.5 Mobilisation

Mobilisation data as expected exhibited distinct steps in turbidity in response to the imposed hydraulic conditions, rather than more gradual or continuous increases. Fig. 8 shows the normalised step changes in turbidity (eqn (3)) as a function of the flow rate imposed. The different lines show the data grouped and sorted with respect to the proceeding hydraulic conditions of the accumulation process. At lower mobilisation flowrates of 0.3 and 0.6 L s^{-1}, turbidity continued to decrease as increases in flowrates did not outweigh accumulation effects thus producing negative changes in turbidity (material continued to accumulate resulting in turbidity decrease).

From Fig. 8 it can be seen that mobilisation following accumulation at zero flow (0 L s^{-1}) is characterised by three distinct parts: (1) a continuous decrease in turbidity until reaching 0.6 L s^{-1}, indicating accumulation outweighing mobilisation effects; (2) a linear increase in turbidity between 0.6 and 1.75 L s^{-1}, indicating mobilisation of sediments; (3) a slower linear increase between 1.75 L s^{-1} and 5 L s^{-1}, indicating mobilisation of cohesive layers. Mobilisation following accumulation at 0.3 and 0.6 L s^{-1} show an initial neutral period, with neither additional accumulation or mobilisation, followed by approximately linear increase. Mobilisation following accumulation at 1.25 L s^{-1} exhibited two linear patterns: (1) increase curtailing after 1.75 L s^{-1}, followed by (2) a shallower increase until 5 L s^{-1}.

To investigate the hydraulic parameter that best quantifies the mobilisation process and to further investigate the patterns of turbidity change during mobilisation the cumulative turbidity change was plotted against shear stress, velocity, and Reynolds number. Shear stress was found to yield the best insights and is shown is Fig. 9. Shear stress showed similar patterns for flow steps following accumulation at 0 and 1.25 L s^{-1}, with a linear increase until 1.75 L s^{-1} (≈0.4 N m^{-2}). However, due to the exponential scaling of shear stress *versus* velocity, material mobilisation now appeared to follow a steeper linear pattern until the mobilisation step of 2.5 L s^{-1} (≈0.75 N m^{-2}) regardless of the preceding accumulation flow.

Table 5 summarises the observed material mobilisation behaviour as a function of shear stress. At lower mobilisation steps of 0.015 and 0.055 N m^{-2}, hydraulic forces were insufficient to result in the mobilisation of accumulated

Table 4 Hydraulic metrics of flow, velocity, Reynolds number and shear stress used to identify hydraulic conditions and explain accumulation processes occurring in networks

Flowrate L s^{-1}	Velocity m s^{-1}	Reynolds Nr ≈ (at 10 C)	Shear stress N m^{-2}	Average turbidity decrease (%)	Average turbidity decrease (NTU)	Best fit line	Inferred accumulation processes
0	0	0	0	20.6	0.26	Exponential	Sedimentation
0.3	0.06	3600	0.015	34.5	0.57	Exponential	Sedimentation dominant, some cohesive layers
0.6	0.12	7200	0.05	28.5	0.32	Exponential	Sedimentation dominant, some cohesive layers
1.25	0.25	15 100	0.21	28.5	0.49	Exponential, linear	Sedimentation and cohesive layers, neither dominant
2.5	0.50	30 300	0.77	10.2	0.14	Linear	Cohesive layers
5	1.00	60 600	2.77	4	0.06	Linear	Cohesive layers

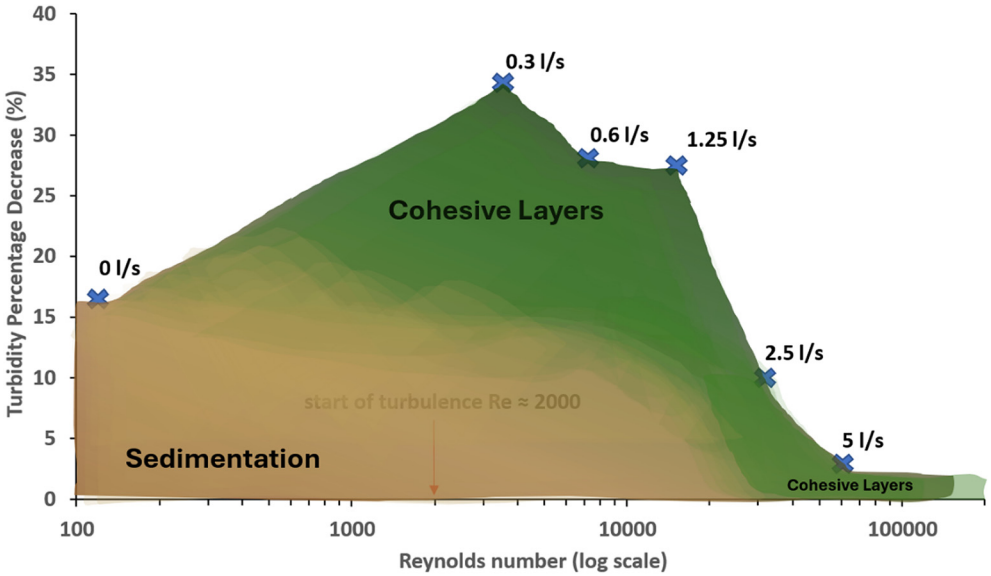

Fig. 7 Experimental data points and conceptual shading for when sedimentation and cohesive layer processes occurred. Note log scaling of Reynolds number on *x*-axis.

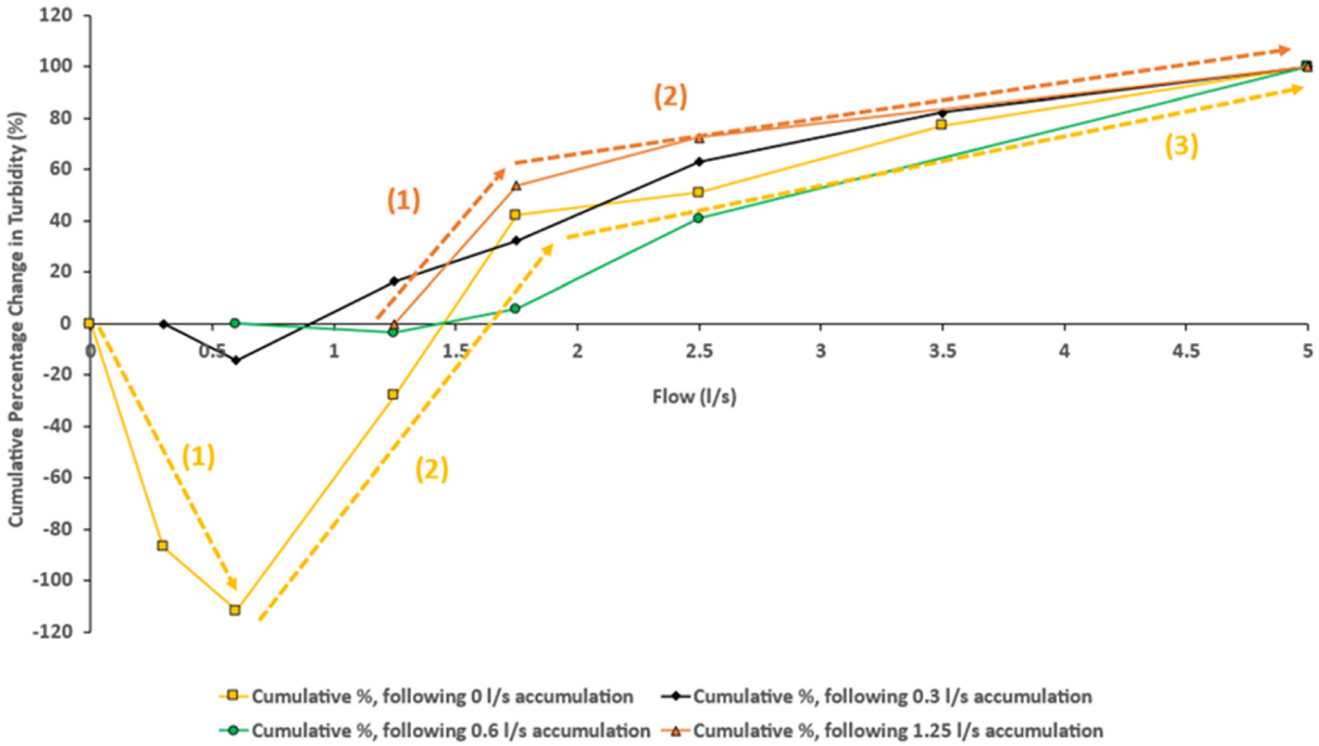

Fig. 8 Patterns of cumulative percentage change in turbidity as a function of flow steps. Arrows and numbers reference the description of the observed behaviour in the text.

material. As the hydraulic conditions in the pipe are turbulent (Re > 3600), mobilisation does not seem to be caused simply by the transition into turbulence conditions. Mobilisation of sediments is observed to be dominant starting around 0.21 N m^{-2} (1.25 L s^{-1}) and dominating until 0.4 N m^{-2} (1.75 L s^{-1}) to 0.75 N m^{-2} (2.5 L s^{-1}). As well as providing the best insight into the collected data, shear stress captures pipe diameter and roughness effects, which are reported to effect particle shielding and cohesion,[7] and is a measure of force. Shear stress is therefore recommended as the hydraulic measure to describe mobilisation processes.

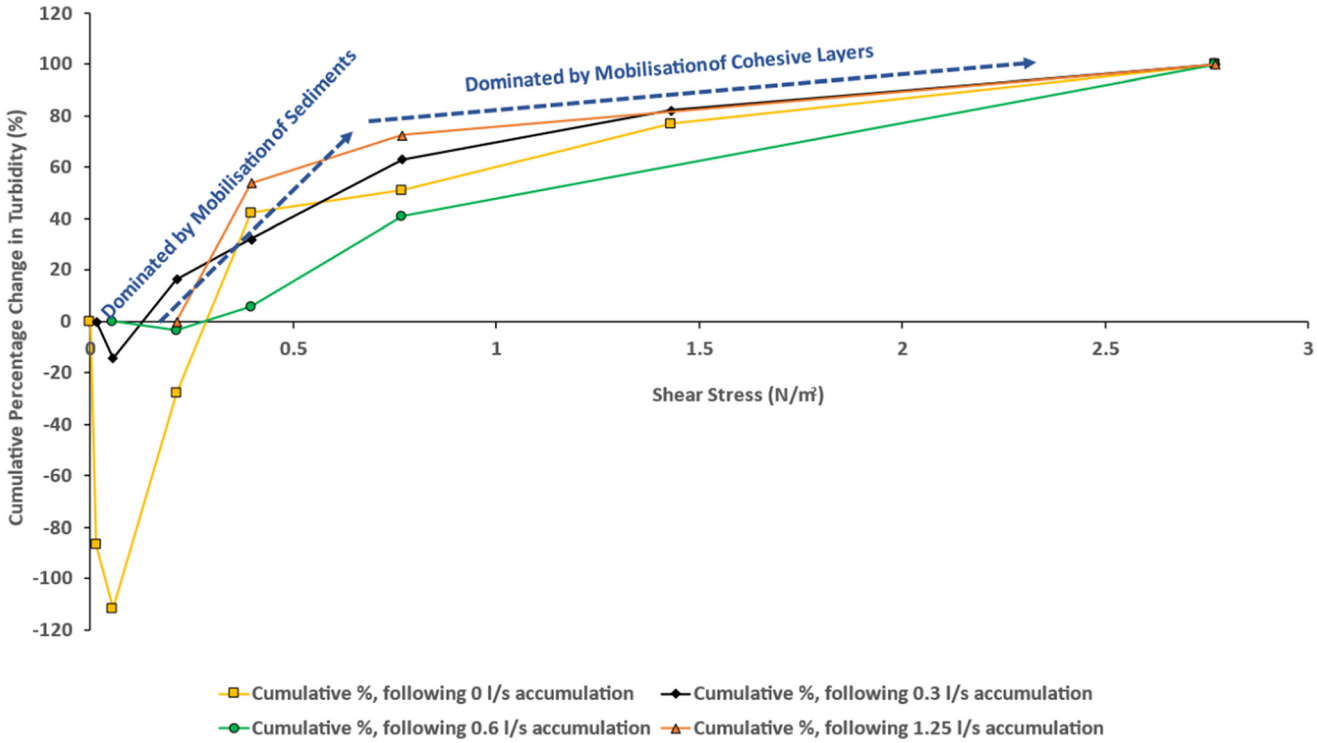

Fig. 9 Patterns of cumulative percentage change in turbidity as a function of shear stress. Blue arrows and annotated text describe the dominant material type mobilised.

Table 5 Hydraulic metrics of flow, velocity, Reynolds number and shear stress used to identify hydraulic conditions and explain mobilisation processes

Flowrate L s^{-1}	Shear stress N m^{-2}	Proposed mobilised material
0.3	0.015	No mobilisation, accumulation dominating
0.6	0.05	No mobilisation, accumulation dominating
1.25	0.21	Some mobilisation of sediments which dominate the response
1.75	0.40	Mobilisation of sediments dominate the response
2.5	0.76	Mobilisation of sediments dominate the response
3.5	1.43	Response dominated by mobilisation from cohesive layers
5	2.77	Response dominated by mobilisation from cohesive layers

5. Discussion

Discolouration material behaviour is now being acknowledged as involving both sedimentation and cohesive layer processes and this laboratory research uniquely considers both occurring simultaneously. This represents a significant advance beyond the previous practice where cohesive layers and sedimentation were studied and considered to occur separately. For example, research in the UK focusing on trunk mains observed cohesive layers due to higher shear stresses,[1,14] offering an incomplete view of particle processes. In the Netherlands, research focused on downstream areas with lower Reynolds number and hence sediment dominated behaviour,[16,29] leading to bias towards sedimentation and underestimation of risk where cohesive layers dominate. A more integrated qualitative understanding of discolouration behaviour within networks was recently published highlighting the two processes and that effective discolouration management requires appreciation of when or where each dominates.[4] The quantification of hydraulic conditions by the most informative parameter identified through the laboratory research reported here advances this qualitative research; it provides knowledge and understanding of how best to quantify the hydraulic conditions for operational and modelling applications.

In the analysis and interpretation of results, and in the following discussion, the identification of thresholds that are indicative of the change between dominant processes has been attempted. However, it should be noted a more gradual transition between the dominance of processes is expected as a function of network and material characteristics and this is captured in the conceptual colour coding in Fig. 7. It should also be noted that the results are from a low roughness small diameter pipe; further work is required to confirm the wider

applicability (other pipe material, diameter *etc.*) of the findings reported here.

Analysis of the laboratory data showed material accumulation to be best described by Reynolds number (Table 4) as it captures turbulence effects. Turbulence impacts particle movement by introducing forces in addition to buoyancy and drag that counteract particle self-weight and mitigate sedimentation. Turbulence also promotes particles coming in contact with the pipe wall and drives nutrient supply into boundary layer for biofilm growth thus promoting formation of cohesive layers.[8,22] Previous literature on sedimentation has focused on velocity thresholds for describing accumulation.[1,6] Velocity however, does not fully capture potential interactions between self-weight forces and turbulence or changes in forces transporting material into the boundary layer. This research indicates that Reynolds number, by capturing these interactions, is the most informative hydraulic metric to define when accumulation by cohesive layers or sedimentation, dominates.

This laboratory research found shear stress to be most able to describe the particle-flow interactions of mobilisation processes (Fig. 9 and Table 5). While shear stress has been previously used to describe the daily conditioning and mobilisation of cohesive layers of different strength layers,[9,14,19,21] it has not been used to describe the mobilisation of sediments with velocity thresholds previously used.[6,16,26] Velocity only describes the motion of the fluid, it fails to account for pipe roughness effects and does not indicate the magnitude of force exerted (on particles) at pipe walls. This is also consistent with prior research that has suggested additional forces such as inter-particle or particle shielding must be overcome for sediment mobilisation within DWDS.[7,17,28] This research demonstrated that shear stress can be used to identify the mobilisation processes, and it conceptually considers such additional retention forces present between sediments.

A Reynolds number of 3600 (0.06 m s^{-1}), resulted in the fastest accumulation observed in these experiments whilst sedimentation processes dominated accumulation behaviour up to Re 15 100. The threshold of 0.06 m s^{-1} is of particular interest, as mixed results have been reported in the literature regarding this velocity threshold, with some research suggesting that hydraulic conditions of similar low velocities (0.05–0.07 m s^{-1}) prevent sedimentation.[1,6,28,36] Other research, such as by Blokker *et al.*[16] and Poças *et al.*,[18] observed accelerated accumulation at low velocities compared to stagnation either during flushing or laboratory trials respectively, but did not explain why. The results from this laboratory research suggest that pipes, or pipe sections, with low but continuous flows, may be more susceptible to increased discolouration risk due to enhanced accumulation with concurrent cohesive layer and sedimentation processes (if daily peak hydraulic conditions are insufficient to mobilise accumulating material).

The hydraulic condition of ≈0.8 N m^{-2} (Fig. 8) identified by this research as beyond which the rate of material mobilisation was observed to be reduced, aligns with other experimental and field-based research reporting exhaustion of material layers within DWDS or mobilisation of cohesive marine sediments of similar size between 0.5 N m^{-2} to 1.2 N m^{-2}.[19,25,37] However, given that higher shear stresses are reported to continue mobilising cohesive layer material,[21] an operational focus should be to understand which accumulation process dominates and then apply an appropriate management strategy.[4] This research presents the first evidence of a defined operational flushing value (≈0.8 N m^{-2}, 0.5 m s^{-1}) to mobilise sediments in downstream areas of the network (although limited to plastic pipes and not proven in field conditions).

6. Conclusions

This research investigated drinking water distribution system material accumulation and mobilisation processes using controlled laboratory experiments. The experiments used a full-scale pipe loop system and discolouration material collected from operational networks which was introduced to the pipe loop at low yet realistic concentrations. This research acknowledges the simultaneous occurrence of sedimentation and cohesive layers processes and identifies and quantifies under what hydraulic conditions each occurs and hence where and when they dominate.

Findings show that Reynolds number best describes accumulation behaviour and that shear stress best describes mobilisation behaviour. This research found that sedimentation processes tended to dominate accumulation behaviour up to around Re 15 100 (1.25 L s^{-1}, 0.25 m s^{-1}, 0.213 N m^{-2}), beyond which cohesive layers started to dominate. Material was observed to accumulate fastest at Re 3600 (0.3 L s^{-1}, 0.06 m s^{-1}, 0.015 N m^{-2}), likely due to optimal turbulence for simultaneous accumulation processes of sedimentation and cohesive layers plus a continual supply of material (compared to zero flowrate).

Mobilisation was observed to be a function of both the preceding accumulation conditions (material accumulated under stronger hydraulic conditions needed greater forces to mobilise them) and the magnitude of the increase in shear stress. Mobilisation of sediments was observed to start at 0.21 N m^{-2} (0.25 m s^{-1}, Re 15 100) and dominated the turbidity response up to around 0.8 N m^{-2} (0.5 m s^{-1}, Re 30 300). Cohesive layer material was mobilised beyond 0.8 N m^{-2}. The dominance of sediment mobilisation up to around 0.8 N m^{-2} signifies a point of diminishing return that should inform the targeting of flushing flowrates to efficiently mitigate discolouration risk where settling is the dominant accumulation process.

Author contributions

Reinar Lokk: conceptualization, methodology, formal analysis, investigation, writing – original draft, writing – review & editing, visualization. Joby Boxall: conceptualization, writing – review & editing, supervision, funding acquisition.

Stewart Husband: conceptualization, writing – review & editing, supervision, funding acquisition, project administration.

Conflicts of interest

There are no conflicts to declare.

Abbreviations

DWDS	Drinking water distribution systems
EPS	Extracellular polymeric substances
HDPE	High density polyethylene (pipe material)
PE	Polyethylene (pipe material)
NTU	Nephelometric turbidity units
UK	United Kingdom
Sn (S1)	Used to denote experimental stage nr (stage 1)
Rn (R1)	Used to denote experimental repeat or run nr (run 1)
SSC	Suspended solids concentration
TO	Turnover
mg	Milligram
kg	Kilogram
μm	Micrometre
Hr	Hour (time)
τ	Shear stress (N m^{-2})
g	Acceleration due to gravity (m s^{-2})
D	Pipe diameter (m)
S_0	Hydraulic radius (dimensionless)
Re	Reynolds number (dimensionless)

Data availability

The raw data supporting the findings of this study are available in the University of Sheffield data repository at https://doi.org/10.15131/shef.data.31157800.

Acknowledgements

This work was supported by United Utilities and the WIRe Centre for Doctoral Training (UKRI EPSRC EP/S023666/1). For the purpose of open access, the author has applied a creative commons attribution (CC BY) license to any author accepted manuscript versions arising.

References

1 J. H. Vreeburg and J. B. Boxall, Discolouration in potable water distribution systems: a review, *Water Res.*, 2007, **41**, 519–529.
2 C. Cartier, R. B. Arnold Jr, S. Triantafyllidou, M. Prévost and M. Edwards, Effect of flow rate and lead/copper pipe sequence on lead release from service lines, *Water Res.*, 2012, **46**, 4142–4152, DOI: 10.1016/j.watres.2012.05.049.
3 A. S. Braga, R. Saulnier, Y. Filion and A. Cushing, Dynamics of material detachment from drinking water pipes under flushing conditions in a full-scale drinking water laboratory system, *Urban Water J.*, 2020, **17**, 745–753, DOI: 10.1080/1573062X.2020.1800759.
4 J. Boxall, M. Blokker, P. Schaap, V. Speight and S. Husband, Managing discolouration in drinking water distribution systems by integrating understanding of material behaviour, *Water Res.*, 2023, **243**, 120416, DOI: 10.1016/j.watres.2023.120416.
5 J. Ackers, M. Brandt and J. Powell, *Hydraulic characterisation of deposits and review of sediment modelling*, UK Water Industry Research Ltd, London, 2001.
6 G. Ryan, P. Mathes, G. Haylock, A. Jayaratne, J. Wu, N. Noiu-Mehidi, C. Grainger and B. V. Nguyen, *Particles in water distribution systems: characterisation of particulate matter in drinking water supplies*, Cooperative Research Centre for Water Quality and Treatment, Australia, 2008.
7 A. S. Braga and Y. Filion, Initial stages of particulate iron oxide attachment on drinking water PVC pipes characterised by turbidity data and brightfield microscopy from a full-scale laboratory, *Environ. Sci.: Water Res. Technol.*, 2022, **8**, 1195–1210, DOI: 10.1039/D2EW00010E.
8 J. Boxall, P. J. Skipworth and A. J. Saul, A novel approach to modelling sediment movement in distribution mains based on particle characteristics, in *Computing and Control for the Water Industry*, Leicester, UK, 2001.
9 P. S. Husband, J. B. Boxall and A. J. Saul, Laboratory studies investigating the processes leading to discolouration in water distribution networks, *Water Res.*, 2008, **42**, 4309–4318.
10 P. S. Husband and J. B. Boxall, Understanding material accumulation and discolouration risk in distribution networks, in *Proceedings of the 1st International WDSA Conference*, Kingston, Ontario, Canada, 2018.
11 E. J. M. Blokker and E. J. Pieterse-Quirijns, Modeling temperature in the drinking water distribution system, *J. AWWA*, 2013, **105**, E19–E28, DOI: 10.5942/jawwa.2013.105.0011.
12 L. Zlatanovic, J. P. van der Hoek and J. H. G. Vreeburg, An experimental study on the influence of water stagnation and temperature change on water quality in a full-scale domestic drinking water system, *Water Res.*, 2017, **123**, 761–772, DOI: 10.1016/j.watres.2017.07.019.
13 K. Fish, P. S. Husband and J. B. Boxall, The impact of chlorine concentration on the discolouration response of biofilms in drinking water distribution systems, in *Proceedings of the 1st International WDSA/CCWI Joint Conference*, Kingston, Ontario, Canada, 2018.
14 S. Husband, K. E. Fish, I. Douterelo and J. Boxall, Linking discolouration modelling and biofilm behaviour within drinking water distribution systems, *Water Sci. Technol.: Water Supply*, 2016, **16**, 942–950, DOI: 10.2166/ws.2016.045.
15 K. Fish, A. M. Osborn and J. B. Boxall, Biofilm structures (EPS and bacterial communities) in drinking water distribution systems are conditioned by hydraulics and influence discolouration, *Sci. Total Environ.*, 2017, **593–594**, 571–580, DOI: 10.1016/j.scitotenv.2017.03.176.
16 E. J. Blokker, J. H. Vreeburg, P. G. Schaap and J. C. van Dijk, The self-cleaning velocity in practice, in *Water Distribution Systems Analysis 2010*, Tucson, USA, 2010.
17 A. S. Braga and Y. Filion, The interplay of suspended sediment concentration, particle size and fluid velocity on the rapid deposition of suspended iron oxide particles in

PVC drinking water pipes, *Water Res.: X*, 2022, **15**, 100143, DOI: 10.1016/j.wroa.2022.100143.

18 A. Poças, N. Rebola, S. Rodrigues, M. J. Benoliel, L. Rietveld, J. Vreeburg and J. Menaia, Pilot studies on discolouration loose deposits' build-up, *Urban Water J.*, 2014, **12**, 631–638.

19 S. Husband and J. B. Boxall, Field studies of discoloration in water distribution systems: model verification and practical implications, *J. Environ. Eng.*, 2010, **136**, 86–94, DOI: 10.1061/(ASCE)EE.1943-7870.0000115.

20 S. Husband and J. Boxall, Understanding and managing discolouration risk in trunk mains, *Water Res.*, 2016, **107**, 127–140.

21 R. L. Sharpe, C. A. Biggs and J. B. Boxall, Hydraulic conditioning to manage potable water discolouration, *Proceedings of the Institution of Civil Engineers - Water Management*, 2019, **172**(1), 3–13.

22 P. van Thienen, J. H. Vreeburg and E. J. Blokker, Radial transport processes as a precursor to particle deposition in drinking water distribution systems, *Water Res.*, 2011, **45**, 1807–1817, DOI: 10.1016/j.watres.2010.11.034.

23 A. S. Braga and Y. Filion, A novel monitoring scheme to detect iron oxide particle deposits on the internal surface of PVC drinking water pipes, *Environ. Sci.: Water Res. Technol.*, 2021, **7**, 2116–2128, DOI: 10.1039/D1EW00614B.

24 E. J. Blokker, P. G. Schaap and J. H. G. Vreeburg, Comparing the fouling rate of a drinking water distribution system in two different configurations, in *Proceedings of the 11th International Conference on Computing and Control for the Water Industry*, University of Exeter, Exeter, UK, 2011.

25 D. M. Cook and J. B. Boxall, Discoloration material accumulation in water distribution systems, *J. Pipeline Syst. Eng. Pract.*, 2011, **2**, 113–122.

26 E. J. Blokker, J. Vreeburg, P. G. Schaap and P. Horst, Self-cleaning networks put to the test, in *World Environmental and Water Resources Congress 2007: Restoring Our Natural Habitat*, ASCE, 2007.

27 I. Sunny, P. S. Husband and J. B. Boxall, Impact of hydraulic interventions on chronic and acute material loading and discolouration risk in drinking water distribution systems, *Water Res.*, 2020, **169**, 115224.

28 I. W. M. Pothof and E. J. M. Blokker, Dynamic hydraulic models to study sedimentation in drinking water networks in detail, *Drinking Water Eng. Sci.*, 2012, **5**, 87–92, DOI: 10.5194/dwes-5-87-2012.

29 J. H. G. Vreeburg, E. J. M. Blokker, P. Horst and J. C. van Dijk, Velocity-based self-cleaning residential drinking water distribution systems, *Water Sci. Technol.: Water Supply*, 2009, **9**, 635–641.

30 K. E. Fish, N. Reeves-McLaren, S. Husband and J. Boxall, Unchartered waters: the unintended impacts of residual chlorine on water quality and biofilms, *npj Biofilms Microbiomes*, 2020, **6**, 34, DOI: 10.1038/s41522-020-00144-w.

31 E. I. Prest, P. G. Schaap, M. D. Besmer and F. Hammes, Dynamic hydraulics in a drinking water distribution system influence suspended particles and turbidity, but not microbiology, *Water*, 2021, **13**, 109, DOI: 10.3390/w13010109.

32 P. S. Husband and J. B. Boxall, Asset deterioration and discolouration in water distribution systems, *Water Res.*, 2011, **45**, 113–124, DOI: 10.1016/j.watres.2010.08.021.

33 B. B. Weiner, *What is particle size distribution weighting: how to get fooled about what was measured and what it means?*, Brookhaven Instruments Corporation, 2011.

34 A. Rawle, *Basic principles of particle size analysis*, 2020.

35 J. B. Boxall and A. J. Saul, Modeling discoloration in potable water distribution systems, *J. Environ. Eng.*, 2005, **131**, 716–725.

36 P. G. Schaap, Flow related turbidity distribution over the height of a main, in *Proceedings of the 1st International WDSA/CCWI Joint Conference*, Kingston, Canada, 2018.

37 L. C. van Rijn, Unified view of sediment transport by currents and waves. I: initiation of motion, bed roughness, and bed-load transport, *J. Hydraul. Eng.*, 2007, **133**, 649–667, DOI: 10.1061/(ASCE)0733-9429(2007)133:6(649).